

# We are IntechOpen, the world's leading publisher of Open Access books Built by scientists, for scientists

6,900

Open access books available

186,000

International authors and editors

200M

Downloads

Our authors are among the

154

Countries delivered to

TOP 1%

most cited scientists

12.2%

Contributors from top 500 universities



WEB OF SCIENCE™

Selection of our books indexed in the Book Citation Index  
in Web of Science™ Core Collection (BKCI)

Interested in publishing with us?  
Contact [book.department@intechopen.com](mailto:book.department@intechopen.com)

Numbers displayed above are based on latest data collected.  
For more information visit [www.intechopen.com](http://www.intechopen.com)



# Radiation Exchange at Greenhouse Tilted Surfaces under All-Sky Conditions

*Erick K. Ronoh*

## Abstract

Greenhouses generally exhibit a greater degree of thermal radiation interaction with the surroundings than other buildings. A number of greenhouse thermal environment analyses have handled the thermal radiation exchange in different ways. Thermal radiation exchange at greenhouse surfaces is of great interest for energy balance. It dominates the heat transfer mechanisms especially between the cover material surface and the surrounding atmosphere. At these surfaces, the usual factors of interest are local temperatures and energy fluxes. The greenhouse surfaces are inclined and oriented in various ways and thus can influence the radiation exchange. The scope of this work is determination of the thermal radiation exchange models as well as effects of surface inclination and orientation on the radiation exchange between greenhouse surfaces and sky. Apart from the surface design and the thermal properties of the cover, the key meteorological parameters influencing longwave and shortwave radiation models were considered in detail. For the purpose of evaluating surface inclination and orientation effects, four identical thermal boxes were developed to simulate the roof and wall greenhouse surfaces. The surface temperatures and atmospheric parameters were noted under all-sky conditions (clear-sky and overcast). Differences in terms of surface-to-air temperature differences at the exposed roof and wall surfaces as influenced by surface inclination and orientation are discussed in this work. Overall, the findings of this work form a basis for decisions on greenhouse design improvements and climate control interventions in the horticultural industry.

**Keywords:** Radiation exchange, Greenhouses, Tilted surfaces, Roof, Wall, Sky

## 1. Introduction

Thermal radiation dominates the heat transfer mechanisms especially between the cover material surface and the surrounding atmosphere. The radiation heat transfer depends on the orientation of the surfaces relative to each other as well as their radiation properties and temperatures [1]. For a non-horizontal surface (e.g. roof and wall), the radiation exchange between the surface and the sky is weighted by a view factor. The view factor gives the fraction of the view from a base surface obstructed by a given other surface [2]. Generally, single-span greenhouses are oriented such that the length runs east–west. This orientation maximizes winter sunlight and heat gain in the greenhouse [3]. Gutter-connected greenhouses are



**Figure 1.**  
*Multi-span Venlo glass greenhouse in Hannover, Germany.*

oriented with the length running north–south (**Figure 1**). According to Sanford [3], this ensures that the shadow cast by the gutters moves during the day. If the orientation is east–west in this case, the shadow of the gutter will move very little, resulting in less direct sunlight and thus slowing down the plant growth. Spatial irregularities of irradiance with east–west oriented greenhouses could often be a problem at all latitudes [4]. Generally, a specific orientation is suitable for a given purpose and location.

The precise determination of the radiation components is essential for a good estimate of the net radiation balance and, consequently, of the radiation and energy balances [5]. The radiation balance, the main source of energy available for the physical and biological processes, is the essential component of the energy balance at the surface. With the availability of hydro-meteorological data such as air temperature, relative humidity, and cloudiness, the longwave radiation can be estimated for any location and at any given time. The understanding of the factors which control the ascending and descending flows in the atmosphere is essential to improve the models used in the various environmental applications [6].

Internationally, a substantial emphasis is placed on a greenhouse orientation that maximizes light interception. At different surface inclinations and orientations, accurate radiation data and models are required for the longwave radiation exchange at representative conditions [7]. Hence, this chapter seeks to determine the influence of the glass-covered greenhouse surface inclination and orientation on the exterior longwave radiation exchange.

## **2. Thermal radiation exchange at greenhouse surfaces**

Generally, there is greater thermal radiation interaction between greenhouses and the surroundings compared to other buildings. As a result, thermal radiation loss can particularly become the dominant mechanism of total heat loss especially at night. Thermal radiation is therefore a very important factor in determining the thermal environment inside a greenhouse. Simulation models help to address the challenges related to the high costs of directly measuring longwave radiation. The simulation models further allow the estimation of the thermal exchange on any building surfaces. It is evident from the models that neglecting to consider thermal radiation (shortwave and longwave) exchange in sufficient detail can lead

to serious inaccuracies in the model predictions. For the energy balance under day-time conditions, the solar irradiance on greenhouse surfaces plays a very important role and should, therefore, be accounted for precisely. The solar radiation data is readily available from most weather stations particularly for horizontal surfaces and this, together with other parameters, can be utilized in calculating the total irradiance on tilted surfaces with an acceptable accuracy. Knowledge of the thermal radiation exchange is vitally important for numerous applications in agriculture requiring surface radiation and energy balance.

## 2.1 Longwave radiation exchange

Modeling of longwave radiation exchange between the outside surfaces and the sky requires the knowledge of the sky temperature [8]. The equivalent sky temperature  $T_{sky}$  has been estimated differently by various researchers. The common equations applied in the  $T_{sky}$  computation are empirical in nature and are related to the air temperature. Thus, they perform best for areas with a radiative climate similar to the one for which they were originally obtained. Hence, the available model by von Elsner [9] was selected since it was developed within the same study location. Other than the air temperature, this model utilizes a cloudiness factor as an important factor in the  $T_{sky}$  estimation. Thus, for all-sky conditions,  $T_{sky}$  was expressed by Eq. (1) [9]:

$$T_{sky} = \{1.2 T_o - 21.4 + C(20.6 - 0.26T_o)\} + 273.15 \quad (1)$$

Sky conditions were modeled on the basis of the cloudiness factor  $C$ , which is a very important parameter in the longwave radiation exchange. Cloudiness greatly affects the magnitude of downwelling longwave radiation received at the surface of the earth. Therefore, cloudiness should be considered while modeling the downwelling longwave radiation.

A computer vision-based algorithm was developed in Halcon 11.0 (HALCON 11.0.3, 2012) which identified selected regions of interest on the weather maps and calculated the cloudiness situation at a given location, thus yielding a cloudiness factor  $C$  (**Figure 2**). Halcon is generally a comprehensive standard software for machine vision with an integrated development environment that is used worldwide.

The weather maps were obtained from the web-service Weather Online (WetterOnline). Within a given region, the weather map shows the cloud cover intensity and distribution. It also shows whether rain or snow is falling. Cloudiness influences the longwave radiation emitted by the atmosphere downward to the earth's surface.

For all-sky conditions, the downwelling longwave radiation  $LWR_d$  has the general form given by Eq. (2) [10, 11]:

$$LWR_d = \varepsilon_a \sigma T_a^4 \quad (2)$$

The  $\varepsilon_a$  formulation has the basic structure expressed by Eq. (3) [5]:

$$\varepsilon_a = \varepsilon_{cs} (1 + b C^d) \quad (3)$$

The positive relationship of the radiation with the air temperature and cloudiness indicates that empirical models can be used in the simulation under all-sky conditions.

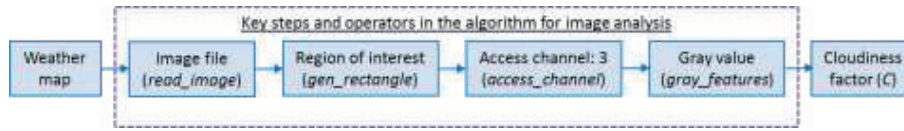


**Figure 2.**  
Procedure overview for the image analysis with Halcon 11.0.

According to Howard and Stull [12], longwave radiation from the surrounding objects such as trees can enhance the total downwelling longwave radiation  $LWR_{d,t}$  and should not be neglected. This is specifically added for comparison with the measurement from the net radiometer.  $LWR_{d,t}$  is therefore expressed by Eq. (4) as:

$$LWR_{d,t} = LWR_d + \varepsilon_{gnd} F_{gnd} \sigma T_a^4 \quad (4)$$

The view factor gives the fraction of the view from a base surface obstructed by a given other surface [2]. It can be calculated numerically or analytically. A horizontal surface can see the whole sky, hence it radiates to the whole sky and its view factor with respect to the sky is equal to one. For a non-horizontal surface (e.g. roof and wall), the view factor has to be used since this is less than one. A vertical surface (tilt angle from the vertical plane =  $0^\circ$ ) will only see half of the sky. The radiation that leaves the inclined surface is either incident on the ground or it goes to the sky (**Figure 3**).

An additional term accounting for the reflected downwelling radiation is incorporated in the computation of the upwelling longwave radiation [13]. From the equations above, the sum of the emitted longwave radiation by the surface  $LWR_u$  and the reflected downwelling longwave radiation gives the total upwelling longwave radiation  $LWR_{u,t}$  [14]. Generally, the upwelling longwave radiation  $LWR_u$  can be computed once the surface temperature  $T_s$  and emissivity  $\varepsilon_s$  are known. The difference in all upwelling radiation and all downwelling radiation must result in  $Q_{s,eff}$ . Thus the  $LWR_{u,t}$  is expressed in the form given by Eq. (5):

$$LWR_{u,t} = LWR_u + (1 - \varepsilon_s) LWR_d = Q_{s,eff} + LWR_d \quad (5)$$

Prediction models provide a more realistic understanding of the thermal radiation exchange between the greenhouse surfaces and the sky if all the required parameters can be accurately determined. The clear-sky atmospheric emissivity parameterizations that include both the near-surface water vapor pressure and the air temperature tend to outperform those consisting of only the air temperature.

Considering an exterior surface and the relevant parameters, the thermal radiation exchange at the surface  $Q_s$  is the sum of the components due to the exchange with the sky, the air and the ground, as expressed in Eq. (6):

$$Q_s = \varepsilon_s \sigma \left\{ \varepsilon_{sky} F_{sky} (T_s^4 - T_{sky}^4) + \varepsilon_a F_{air} (T_s^4 - T_a^4) + \varepsilon_a F_{gnd} (T_s^4 - T_{gnd}^4) \right\} \quad (6)$$

## 2.2 Solar irradiance on tilted surfaces

According to El-Sebaili et al. [15], estimation of total solar radiation incident on tilted surfaces can be expressed by Eq. (7) as:

$$I_{t,t} = I_{b,h} \psi_b + I_{d,h} \psi_d + I_{g,h} \rho_g \psi_r \quad (7)$$

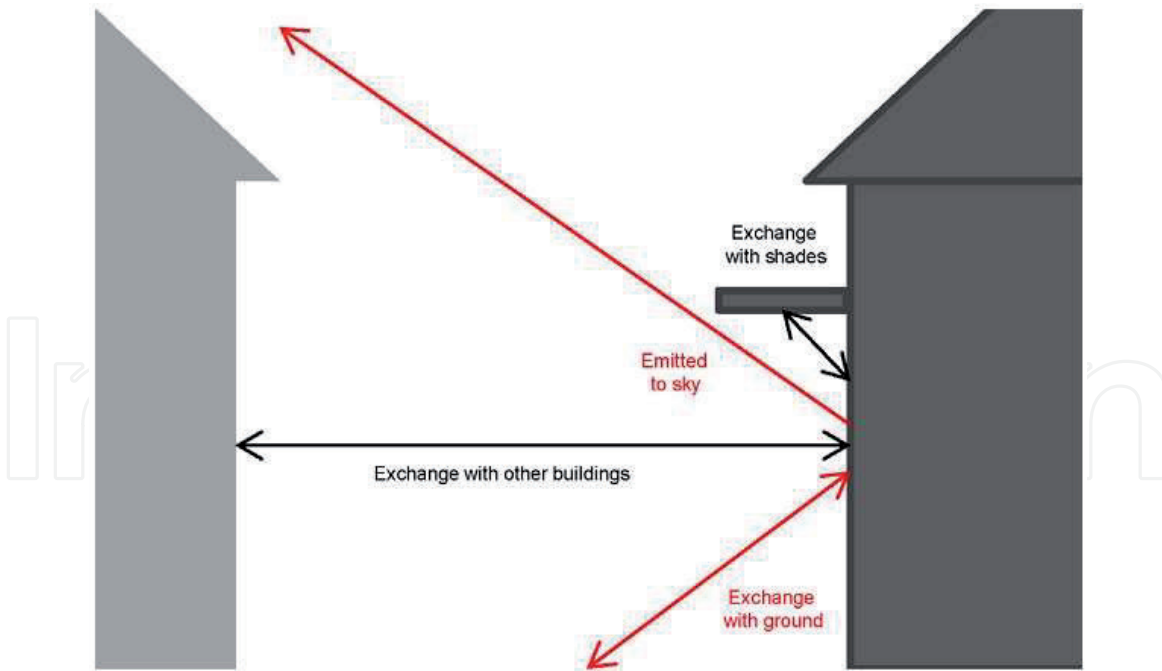


**Figure 3.**  
 Longwave radiation exchange processes at an exterior building surface.

The radiation conversion factors ( $\Psi_b$ ,  $\Psi_d$  and  $\Psi_r$ ) are useful in transforming the horizontal solar radiation components (**Figure 4**) to compute the total solar irradiance on the tilted surfaces.

For a surface with a given orientation, the daily value of  $\Psi_b$  is related to the time variation of incident beam radiation, the intensity of which on the ground level is a function of the atmospheric transmittance. With an angle of incidence  $\vartheta$ , a zenith angle  $\vartheta_z$  and an inclination angle  $\beta$ , the radiation conversion factors are given by Eqs. (8)–(10) [15, 16]:

$$\psi_b = \frac{\cos \theta}{\cos \theta_z} \quad (8)$$

$$\psi_d = \frac{1 - \cos \beta}{2} \quad (9)$$

$$\psi_r = \frac{1 + \cos \beta}{2} \quad (10)$$

### 2.3 Exterior surface energy balance

The energy balance at the exterior greenhouse surface is necessary in order to establish the net radiation gain (daytime solar gain) or the net radiation loss (due to heating at night). The net radiation  $R_n$  is important for surface energy analysis and is generally defined as the difference between incoming and outgoing radiation of both short and long wavelengths [17]. This net (all-wave) radiation  $R_n$  at the surface can be determined as the algebraic sum of the net shortwave radiation  $R_{n,sw}$  and the net longwave radiation  $R_{n,lw}$  [18], given by Eq. (11):

$$R_n = R_{n,sw} + R_{n,lw} \quad (11)$$

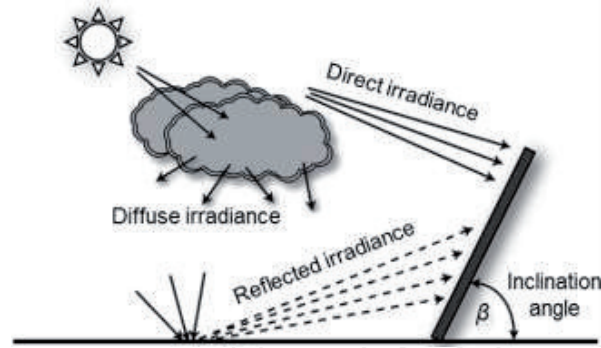


**Figure 4.**  
Components of solar irradiance on tilted surfaces.

This net radiation balance  $R_n$  considers the total solar irradiance and the reflected component for  $R_{n,sw}$ , while the downwelling and the upwelling longwave radiation components are used in the calculation of  $R_{n,lw}$ . Hence, the  $R_n$  is further expressed as (Eq. (12)):

$$R_n = I_{t,t} (1 - \alpha_s) + LWR_{d,t} - LWR_{u,t} \quad (12)$$

During the day, the sun which generally provides a large amount of radiation assures a net gain of energy, because the losses are much smaller. This net gain of energy causes a subsequent greenhouse air temperature rise. However, at night, the warm masses within the greenhouse (earthen floor, concrete paths, metal benches, plants, etc.) produce significant radiation losses to the colder outdoor environment. The net energy loss is caused by the transmission of infrared and thermal radiation through the cover, as well as the emission of radiation from the cover to the cold sky.

Under daytime and nighttime situations, the net radiation of the greenhouse is important for the evaluation of the greenhouse energy situation. It is essentially a measure of the fundamental energy available at greenhouse surfaces. A combination of night sky conditions (e.g. cloudiness, atmospheric emissivity, relative humidity) and the location of adjacent surfaces (such as other greenhouses or buildings) can directly affect the net radiation losses. For a dry greenhouse system (with no plants), energy balance requires knowledge of air exchange rate.

### 3. Greenhouse surface inclination and orientation

Four identical thermal boxes were developed to represent the surfaces of a glass-covered greenhouse. The four boxes were necessary in order to achieve the east, west, north, and south orientations, while changing the inclination angles characterizing the standard Venlo greenhouse surfaces. Each of the developed thermal boxes measured 1.2 m long, 0.95 m wide and 0.6 m high. The base and sidewalls of the boxes were made of Styrodur (BASF, Germany) with a thickness of 10 cm and a lightweight construction. The Styrodur also has excellent insulation properties, high compressive strength, low water absorption and resistance to aging and decay. The initial determination of the air exchange rate due to leaks with a tracer gas [19] proved that the boxes were identical. The errors due to workmanship and closing of the boxes were therefore minimized as much as possible. The exterior surfaces were inclined such that they characterize the roof slope and the walls. Based on the revised German standard for Venlo greenhouses, the roof had an inclination angle

of 24° [20]. As expected, both the side and end walls of the Venlo-type greenhouse design had an angle of 90°.

This approach enabled a proper evaluation of the variations in key parameters at the external surfaces due to varied inclination and orientation. In order to avoid obstructions from buildings and trees, an appropriate rooftop was selected for positioning of miniaturized thermal boxes for assessing surface inclination and orientation effects on thermal radiation exchange (**Figure 5**). The measured parameters included net radiation, air temperature, inside and surface temperatures of the boxes, and wind speeds at different directions [7].

A window heating pad (ProfiPower, axhess GmbH & Co. KG, Hausen, Germany) was attached to the bottom section inside the thermal boxes. It was provided with 12 V DC power and in return supplied about 120 W (10 A, 12 V). The heating pad measured 40 cm by 100 cm and weighed about 0.6 kg. The maximum temperature attained by the heating pad was  $55 \pm 5^\circ\text{C}$  and it had an integrated thermostat for temperature control. A switch-mode DC power supply unit (model 6459, Graupner GmbH & Co. KG, Kirchheim/Teck, Germany) was used. The input voltage was 230 V while the output voltage varied between 5 V and 15 V. The output current was adjustable in the range of 0 A to 20 A. Adjustment of the voltage and ampere knobs gave the needed voltage and current values, respectively. In order to reduce the voltage drop, each DC power supply unit was connected to the heating pad using a twin wire cable of  $6 \text{ mm}^2$  cross-sectional area and approximately 46 m length. To ensure uniform heat distribution within the box, an aluminum sheet was attached firmly to the upper side of the heating pad. The aluminum sheet was 0.98 m long, 0.65 m wide, and 0.003 m thick.

During the measurement period (October 2014 to March 2015), temperature regulation was necessary to ensure that the inside temperatures in all the four thermal boxes were similar at any given time. This regulation was done with the ProfiLab Expert 4.0 program by setting the inside temperature  $T_i$  to 8 K above the ambient air temperature  $T_a$ . The program ensured that the heating pad in the boxes remained heated whenever the interior air temperature dropped below the set-point. With an output current of approximately 8 A from the DC power



**Figure 5.**  
*An arrangement of thermal boxes for surface radiation measurement.*

supply, four modular monostable DIN relays (22 Series DPST-NO, FINDER GmbH, Trebur-Astheim, Germany) were connected in between the ME-UBRE relay box (Meilhaus Electronic GmbH, Alling, Germany) and the power supply units. The DIN relays used are equipped with 20 A, 250 V AC contacts rated at 5000 VA AC1 and are ideal for use in commercial applications including heating, air conditioning, and lighting. They were also suitable for this regulation since their operating temperature range is  $-40$ – $40^{\circ}\text{C}$ .

### 3.1 Surface inclination effects

The variation of surface-to-air temperature difference  $\Delta T_{s-a}$  for both the roof and the wall in the four selected wind speed classes are compared in **Figure 6**. The box plots in each of the four directions (south, west, north, and east) display the variability of  $\Delta T_{s-a}$  as the wind speed increases. For all the box orientations,  $\Delta T_{s-a}$  declined with an increase in wind speed. This trend further shows that the wall  $\Delta T_{s-a}$  was always higher than the roof  $\Delta T_{s-a}$  and this was apparently not influenced by the directions of the thermal boxes [7]. Further tests through an analysis of variance (ANOVA) confirmed an insignificant effect of the orientation on the  $\Delta T_{s-a}$  trend ( $p > 0.05$ ).

Unlike in the big south-facing thermal box where the view factor remained unchanged, the case was different in the miniaturized thermal boxes. By changing the inclination angle  $\beta$ , the view factor is similarly altered [2]. In this respect, when  $\beta$  changes from  $24^{\circ}$  (roof) to  $90^{\circ}$  (wall), the view factor of the exterior surface to the sky  $F_{\text{sky}}$  is reduced while that to the surrounding ground objects  $F_{\text{gnd}}$  is increased. At an inclination angle of  $24^{\circ}$ , the roof is the most exposed component of the greenhouse structure. This in turn led to lower surface-to-air temperature differences  $\Delta T_{s-a}$  of the roofs compared to those of the walls. This implies that the sky-oriented exterior roof surfaces are cooled more than the vertical walls.

However, under an overcast condition, the variation in inclination angles did not show any significant changes ( $p > 0.05$ ) in the net longwave radiation loss. This supports the fact that the radiative heat flux is not well connected to the surface inclination as it merely depends on the temperature difference. As expected, the exposed roof loses more heat to the sky than the walls under clear-sky conditions. The surface of interest represents that of the Venlo greenhouse design where the roof fraction is low. This outcome agrees well with the observation that the nighttime heat loss by longwave radiation affects any building surface whose roof fraction is high. This is equivalent to saying that the sensible heat flux is higher when the roof area is more than the wall area. The reduced roof surface area (an area of

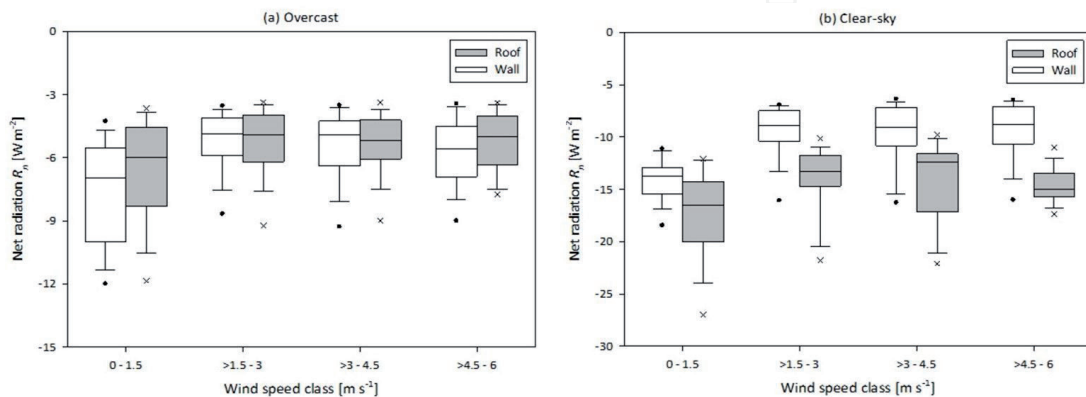


**Figure 6.** Variation of mean net radiation at roof and wall surfaces with wind speed under all-sky conditions: (a) overcast ( $n = 35$  nights), and (b) clear-sky ( $n = 6$  nights).

Surface orientation	Selected wind speed classes [ $\text{m s}^{-1}$ ]			
	0–1.5	> 1.5–3	> 3–4.5	> 4.5–6
South	1.60 <sup>a</sup>	1.49 <sup>b</sup>	0.75 <sup>c</sup>	0.58 <sup>e</sup>
West	1.82 <sup>a</sup>	1.53 <sup>b</sup>	1.14 <sup>d</sup>	1.01 <sup>f</sup>
North	1.63 <sup>a</sup>	1.30 <sup>b</sup>	1.22 <sup>d</sup>	1.13 <sup>f</sup>
East	1.83 <sup>a</sup>	1.41 <sup>b</sup>	1.15 <sup>d</sup>	1.09 <sup>f</sup>
Mean $\pm$ Stdev	1.72 $\pm$ 0.12	1.41 $\pm$ 0.15	1.07 $\pm$ 0.22	0.95 $\pm$ 0.26

(Within column, same letter indicates insignificant differences at 5% level)

**Table 1.** Deviation between wall and roof surface-to-air temperature difference values for different orientations and wind speeds.

major heat loss) in Venlo greenhouses is therefore beneficial in the overall reduction of the heating costs.

### 3.2 Surface orientation effects

For the chosen wind speed classes and surface orientations, the deviation between the surface-to-air temperature difference  $\Delta T_{s-a}$  of the wall and that of the roof was represented by  $\Delta T_{W-R}$ . The values of  $\Delta T_{W-R}$  (in K) are given in **Table 1**. The mean  $\Delta T_{W-R}$  was highest at low wind speed ( $< 1.5 \text{ m s}^{-1}$ ) and lowest at high wind speed ( $> 4.5 \text{ m s}^{-1}$ ). Interestingly, the standard deviation (Stdev) increased with an increase in wind speed, with a range of 0.12 K to 0.26 K. Despite the random orientation of the thermal boxes, the variation in  $\Delta T_{W-R}$  within the same wind speed class did not show a significant difference ( $p > 0.05$ ). For wind speeds  $\geq 3 \text{ m s}^{-1}$ , the south-facing surface registered the lowest values in terms of deviation in  $\Delta T_{s-a}$  unlike the other three surface orientations [7].

Southerly and westerly wind directions were generally dominant during the measurement period. It is also worth noting that the dominant wind speed class was that between  $1.5 \text{ m s}^{-1}$  and  $3 \text{ m s}^{-1}$ . It was also apparent that wind was very variable both in direction and speed. An increase in wind speed reduces the surface resistance; this generally leads to an increased heat loss which is largely brought about by convection.

Based on the trends of the surface-to-air temperature difference  $\Delta T_{s-a}$ , the deviation between the  $\Delta T_{s-a}$  values of the roof and the wall (i.e.  $\Delta T_{W-R}$ ) was not significantly affected by the box orientation. Interestingly, this effect of orientation on nighttime  $R_n$  from this study was insignificant. This indicates that the  $R_n$  was little affected by varying the orientation of the thermal boxes. Generally, these orientations are applicable, especially during the day, in maximizing winter sunlight and heat gain depending on whether the greenhouse is a single-span or a gutter-connected type [3].

## 4. Conclusions

At the greenhouse surfaces, the weighted contributions of thermal emissions from the sky, the surrounding air, and the ground objects are explained by the view factors. During a clear night, the greenhouse surface loses more heat as it radiates to the very cold clear sky. On a regional scale, clouds play a critical role in the radiation balance at the surface. Under both day and night situations, the study delivers

reliable results in terms of the calculation of parameters necessary for the radiation models. The parameters which have an influence on the daytime and nighttime net radiation are surface emissivity, atmospheric emissivity, surface and atmospheric temperatures, and albedo.

With reference to surface inclination and orientation effects, the findings of the study are useful in understanding the impacts of the variously inclined and oriented greenhouse surfaces on heating energy and thus on heat losses. Furthermore, it is important to consider the impact of wind speed specifically for the windward greenhouse surfaces in energy simulations. In this case, the data is distinguished from those of leeward surfaces and the sensitivity to the variation in wind direction can be checked. This becomes more important in uncertainty quantification as a result of variations in the surface orientation.

## Acknowledgements

The author is grateful for the joint scholarship support (between the National Commission for Science, Technology and Innovation (NACOSTI), Kenya and the German Academic Exchange Service (DAAD), Germany) and the material support from Biosystems Engineering Section, Gottfried Wilhelm Leibniz Universität Hannover, Germany.

## Conflict of interest

The author declares that there is no conflict of interest regarding the publication of this chapter.

## Nomenclature

$b, d$	constants determined experimentally [-]
$C$	cloudiness factor [-]
$F_{\text{sky}}$	view factor to the sky [-]
$F_{\text{air}}$	view factor to the air [-]
$F_{\text{gnd}}$	view factor to the ground [-]
$I_{\text{b,h}}$	beam radiation [ $\text{W m}^{-2}$ ]
$I_{\text{d,h}}$	diffuse radiation [ $\text{W m}^{-2}$ ]
$I_{\text{g,h}}$	global radiation on a horizontal surface [ $\text{W m}^{-2}$ ]
$I_{\text{t,t}}$	total solar radiation on the tilted surface [ $\text{W m}^{-2}$ ]
$LWR_{\text{d}}$	downwelling longwave radiation [ $\text{W m}^{-2}$ ]
$LWR_{\text{d,t}}$	total downwelling longwave radiation [ $\text{W m}^{-2}$ ]
$LWR_{\text{u}}$	upwelling longwave radiation [ $\text{W m}^{-2}$ ]
$LWR_{\text{u,t}}$	total upwelling longwave radiation [ $\text{W m}^{-2}$ ]
$Q_{\text{s}}$	thermal radiation exchange [ $\text{W m}^{-2}$ ]
$Q_{\text{s,eff}}$	effective thermal radiation exchange [ $\text{W m}^{-2}$ ]
$R_{\text{n}}$	net (all-wave) radiation [ $\text{W m}^{-2}$ ]
$R_{\text{n,sw}}$	net shortwave radiation [ $\text{W m}^{-2}$ ]
$R_{\text{n,lw}}$	net longwave radiation [ $\text{W m}^{-2}$ ]
$T_{\text{a}}$	air temperature [K]
$T_{\text{gnd}}$	ground temperature [K]
$T_{\text{s}}$	surface temperature [K]
$T_{\text{sky}}$	sky temperature [K]

$\alpha_s$	albedo of the earth surface [-]
$\Delta T_{s-a}$	surface-to-air temperature difference [K]
$\Delta T_{W-R}$	deviation between wall and roof $\Delta T_{s-a}$ values [K]
$\epsilon_{\text{gnd}}$	ground emissivity [-]
$\epsilon_a$	effective atmospheric emissivity [-]
$\epsilon_{\text{cs}}$	clear-sky atmospheric emissivity [-]
$\epsilon_s$	surface emissivity [-]
$\epsilon_{\text{sky}}$	sky emissivity [-]
$\Psi_b$	beam radiation conversion factor [-]
$\Psi_d$	diffuse radiation conversion factor [-]
$\Psi_r$	ground reflected radiation conversion factor [-]
$\rho$	angle of inclination from horizontal [°]
$\rho_g$	ground reflectivity [-]
$\sigma$	Stefan-Boltzmann constant = $5.67 \times 10^{-8}$ [W m <sup>-2</sup> K <sup>-4</sup> ]
$\theta$	angle of incidence [°]
$\theta_z$	zenith angle [°]

IntechOpen

## Author details

Erick K. Ronoh

Department of Agricultural and Biosystems Engineering, Jomo Kenyatta University of Agriculture and Technology, Nairobi, Kenya

\*Address all correspondence to: [ronoh@jkuat.ac.ke](mailto:ronoh@jkuat.ac.ke)

## IntechOpen

© 2021 The Author(s). Licensee IntechOpen. This chapter is distributed under the terms of the Creative Commons Attribution License (<http://creativecommons.org/licenses/by/3.0>), which permits unrestricted use, distribution, and reproduction in any medium, provided the original work is properly cited. 

## References

- [1] Vollebregt HJM, van de Braak NJ. Analysis of radiative and convective heat exchange at greenhouse walls. *Journal of Agricultural Engineering Research*. 1995;**60**(2):99-106. DOI: 10.1006/jaer.1995.1004
- [2] Evins R, Dorer V, Carmeliet J. Simulating external longwave radiation exchange for buildings. *Energy and Buildings*. 2014;**75**:472-482. DOI: 10.1016/j.enbuild.2014.02.030
- [3] Sanford S. Reducing greenhouse energy consumption: An overview. *Energy Efficiency in Greenhouses, Series A3907-01*. University of Wisconsin-Extension, Cooperative Extension. Madison, WI, USA; 2011. 15 p.
- [4] Gupta MJ, Chandra P. Effect of greenhouse design parameters on conservation of energy for greenhouse environmental control. *Energy*. 2002;**27**(8):777-794. DOI: 10.1016/S0360-5442(02)00030-0
- [5] Duarte HF, Dias NL, Maggioletto SR. Assessing daytime downward longwave radiation estimates for clear and cloudy skies in southern Brazil. *Agricultural and Forest Meteorology*. 2006;**139**(3-4):171-181. DOI: 10.1016/j.agrformet.2006.06.008
- [6] Araújo AL, da Silva BB, Braga CC. Simplified modeling of downwelling long-wave radiation over Brazilian semi-arid under irrigation conditions. *Brazilian Journal of Geophysics*. 2012;**30**(2):137-145. DOI: 10.22564/rbgf.v30i2.87
- [7] Ronoh EK, Rath T. Effects of greenhouse surface inclination and orientation on exterior longwave radiation exchange. *Journal of Sustainable Research in Engineering*. 2017;**3**(4):105-112
- [8] Ronoh EK, Rath T. Modelling of longwave radiation exchange at greenhouse surfaces under all-sky conditions. *Agricultural Engineering International: CIGR Journal*. 2015;**17**(4):23-35
- [9] Von Elsner B. Das Kleinklima und der Wärmeverbrauch von geschlossenen Gewächshäusern: Ein Simulationsmodell zur gartenbautechnischen Bewertung unter Berücksichtigung des Einflusses von Standortklima, Pflanzenbestand und Gewächshauskonstruktion. PhD Thesis, Gartenbautechnische Informationen. In: Heft. Vol. 12. Germany: Institut für Technik in Gartenbau und Landwirtschaft, Universität Hannover; 1982
- [10] Choi M, Jacobs JM, Kustas WP. Assessment of clear and cloudy sky parameterizations for daily downwelling longwave radiation over different land surfaces in Florida. USA. *Geophysical Research Letters*. 2008;**35**(L20402):1-6. DOI: 10.1029/2008GL035731
- [11] Dos Santos CAC, Da Silva BB, Rao TVR, Satyamurty P, Manzi AO. Downward longwave radiation estimates for clear-sky conditions over northeast Brazil. *Revista Brasileira de Meteorologia*. 2011;**26**(3):443-450. DOI: 10.1590/S0102-77862011000300010
- [12] Howard R, Stull R. Modeling the downwelling longwave radiation over a groomed ski run under clear skies. *Journal of Applied Meteorology and Climatology*. 2013;**52**(7):1540-1553. DOI: 10.1175/JAMC-D-12-0245.1
- [13] Tang BH, Li ZL. Estimation of instantaneous net surface longwave radiation from MODIS cloud-free data. *Remote Sensing of Environment*. 2008;**112**(9):3482-3492. DOI: 10.1016/j.rse.2008.04.004

[14] Liang SL. Quantitative remote sensing of land surfaces. New Jersey, USA: John Wiley & Sons; 2004 560 p

[15] El-Sebaili AA, Al-Hazmi FS, Al-Ghamdi AA, Yaghmour SJ. Global, direct and diffuse solar radiation on horizontal and tilted surfaces in Jeddah, Saudi Arabia. *Applied Energy*. 2010;**87**(2):568-576. DOI: 10.1016/j.apenergy.2009.06.032

[16] Ronoh EK. Prediction of total solar irradiance on tilted greenhouse surfaces. *Agricultural Engineering International: CIGR Journal*. 2017;**19**(1):114-121

[17] Choi M. Parameterizing daytime downward longwave radiation in two Korean regional flux monitoring network sites. *Journal of Hydrology*. 2013;**476**(1):257-264. DOI: 10.1016/j.jhydrol.2012.10.041

[18] Ayoola MA, Sunmonu LA, Bashiru MI, Jegede OO. Measurements of net all-wave radiation at a tropical location, Ile-Ife, Nigeria. *Atmósfera*. 2014;**27**(3):305-315

[19] Tantau H-J. Heat requirement of greenhouse including latent heat flux. *Landtechnik*. 2013;**68**(1):43-49

[20] Von Elsner B, Briassoulis D, Waaijenberg D, Mistriotis A, von Zabeltitz C, Gratraud J, et al. Review of structural and functional characteristics of greenhouses in European Union countries, Part II: Typical designs. *Journal of Agricultural Engineering Research*. 2000;**75**(2):111-126. DOI: 10.1006/jaer.1999.0512